Optical Clock Recovery Using a Polarization-Modulator-Based Frequency-Doubling Optoelectronic Oscillator

Shilong Pan and Jianping Yao, *Senior Member, IEEE*

***Abstract*—We propose and demonstrate a flexible optical clock recovery scheme using a polarization-modulator-based frequency-doubling optoelectronic oscillator (OEO). The proposed system can extract both prescaled clock and line-rate clock from a degraded high-speed digital signal using only low-frequency devices. A simple theory is developed to study the physical basis of the optical clock recovery. The OEO operation from a free-running mode to an injection-locking mode is investigated. The locking range is quantitatively predicted. An experiment is then implemented to verify the proposed scheme. A prescaled clock at 10 GHz and a line-rate clock at 20 GHz are successfully extracted from a degraded 20 Gb/s optical time-division-multiplexed (OTDM) signal. The locking range and the phase noise performance are also experimentally investigated. Clock recovery from data signals that have no explicit subharmonic tone is also achieved. The proposed system can be modified to extract prescaled clock and line-rate clock from 160 Gb/s data signal using all 40-GHz devices.**

***Index Terms*—Injection locking, optical clock recovery, optical signal processing, optoelectronic oscillator (OEO), polarization modulator (PolM).**

I. Introduction

OPTICAL clock recovery from data signals that are degraded in transmission is essential for optical signal processing in digital communications systems. Clock recovery includes line-rate clock recovery and prescaled clock recovery. The line-rate clock is mainly used for the applications such as 3R (reamplifation, retiming, and reshaping) regeneration [1], [2], format conversion [3], [4], and optical logic gates [5], [6]. The prescaled clock is required for demultiplexing in high-speed optical time-division-multiplexed (OTDM) networks [7]. Line-rate clock recovery from a high-speed digital signal was reported using injection-locked mode-locked lasers [8]–[10], or self-pulsing lasers [11], [12], while prescaled clock recovery was reported using mode-locked lasers [13], [14], phase-locked loops [15], [16], or optoelectronic oscillators (OEOs) [17], [18]. Among these techniques, OEO-based clock recovery is advantageous since it can simultaneously extract both electrical and optical clocks with high spectral purity and highly stable operation. In addition, because an OEO is usually an oscillator with a high Q factor, it can extract the clock from a highly degraded optical signal [18].

An OEO is an optoelectronic feedback loop consisting of an intensity modulator, an optical fiber delay line (or an electrical phase shifter), a photodetector (PD), an electrical amplifier, and an electrical bandpass filter (EBPF) [19]. The net gain of the loop should be greater than unity to ensure that the OEO is able to oscillate. When a continuous-wave (CW) lightwave is injected into the modulator, the OEO will start to oscillate at one of its eigenmodes determined by the center frequency of the EBPF. The spacing between two adjacent eigenmodes is determined by the total length of the loop. If an incoming data signal containing a clock with a frequency near the oscillating frequency is introduced into the OEO loop, the OEO will be injection locked. The clock signal is then extracted while other frequency components in the data signal are suppressed.

Generally, an OEO can operate at a maximum frequency that is limited by the bandwidth of the electro-optic modulator and the PD. As a result, an OEO is usually used for prescaled clock recovery to lock the residual subharmonic (SH) tones in a high-speed OTDM data train. To obtain a high-speed line-rate clock, a pulse compressor and an external time-division multiplexer must be used [20], making the system complicated and costly. To extend the operational frequency, frequency-doubling OEOs have been proposed [21]–[24]. Sakamoto *et al.* suggested a frequency-doubling OEO by biasing a $LiNbO_3$ Mach-Zehnder modulator (MZM) at the minimum transmission point (MITP) [21]. This frequency-doubling OEO was further applied for optical clock recovery [22], showing a potential solution to extract an optical prescaled clock from a high-repetition-rate data signal using low-frequency devices. The major limitation of the approaches in [21], [22] is that a high-frequency electrical amplifier and an electrical frequency divider are needed to obtain the feedback signal required for the optoelectronic oscillation, which makes the OEO operate only at a relatively low frequency. By using the wavelength-dependent nature of the half-wave voltage of a $LiNbO_3$ MZM, Shin *et al.* proposed an approach to generating a frequency-doubled microwave signal using a self-starting OEO [23]. In the system, two CW lasers operating at 1550 and 1310 nm were used. The bias voltage of the MZM was carefully adjusted such that the modulation was performed at the quadrature transmission point (QTP) for the wavelength at 1310 nm to produce a low-frequency feedback signal, and the modulation was performed at the MITP for the wavelength at 1550 nm to generate a

Manuscript received January 12, 2009; revised April 10, 2009. First published April 28, 2009; current version published July 24, 2009. This work was supported by the Natural Sciences and Engineering Research Council of Canada (NSERC).

The authors are with the Microwave Photonics Research Laboratory, School of Information Technology and Engineering, University of Ottawa, Ottawa, ON K1N 6N5, Canada (e-mail: jpyao@site.uOttawa.ca).

Color versions of one or more of the figures in this paper are available online at http://ieeexplore.ieee.org.

Digital Object Identifier 10.1109/JLT.2009.2021563

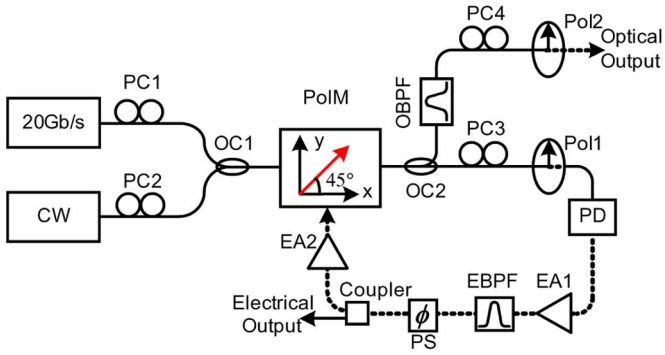

Fig. 1. Schematic diagram of the proposed clock recovery subsystem using a PolM-based frequency-doubling OEO. CW: continuous wave; PC: polarization controller; OC: optical coupler; PolM: polarization modulator; OBPF: optical bandpass filter; Pol: polarizer; PD: photodetector; EA: electrical amplifier; EBPF: electrical bandpass filter; PS: phase shifter.

frequency-doubled signal. The key limitation associated with the operation of an MZM at the MITP is the bias drifting problem, which makes the system unstable or a sophisticated control circuit is needed to stabilize the operation. In addition, two optical sources at two wavelengths are needed, making the system more complicated and costly.

We have recently reported a simple frequency-doubling OEO without the need for high frequency electrical devices and an additional optical light source [24]. In the system, a polarization modulator (PolM) in combination with two optical polarizers connected via two polarization controllers (PCs) is used to operate as a dual-output intensity modulator. One output of the intensity modulator is connected to the RF port of the PolM, to form an optoelectronic loop for the generation of a microwave signal with the fundamental frequency determined by the center frequency of a narrow-band electronic filter. The other output of the intensity modulator provides a fundamental or frequency-doubled optical microwave signal depending on the static phase term introduced by the PC before the polarizer. Because no dc bias is actually required, the system is free from bias drifting problem, ensuring a stable operation. Notice that the system can also be modified to operate as a frequency-quadrupling OEO.

In this paper, a theoretical as well as an experimental study on the use of the PolM-based frequency-doubling OEO for clock recovery is performed. The key advantage of the proposed approach is that the system has the capability of extracting both prescaled and line-rate clocks from a high-speed degraded optical signal using only low frequency devices.

The paper is organized as follows. In Section II, we first describe the PolM-based frequency-doubling OEO and study the physical basis for optical clock recovery. The OEO operation from a free-running mode to an injection-locking mode is investigated. In addition, a simple theory for the analysis of the steady state of an injection-locked OEO is presented. Based on the theoretical analysis, a quantitative prediction for the locking range is derived. In Section III, an experiment is performed. We experimentally extract a prescaled clock at 10 GHz and a line-rate clock at 20 GHz from a 20 Gb/s degraded OTDM signal. The locking range and the phase noise performance are investigated. Furthermore, a prescaled clock at 6.2 GHz and a line-rate clock at 12.4 GHz are also successfully extracted from a 12.4-Gb/s signal that has no explicit SH tone. A conclusion is drawn in Section IV.

II. Theory

The schematic diagram for clock recovery using a PolM-based frequency-doubling OEO is shown in Fig. 1. A small CW light wave at λ_1 from a laser diode and a large OTDM data signal at λ_2 with a data rate of $2\omega_0$ are fiber coupled to a PolM via two PCs (PC1 and PC2). The incident light waves are oriented at an angle of 45° to one principal axis of the PolM. The PolM is connected by two polarizers (Pol1 and Pol2) via two other PCs (PC3 and PC4), which is equivalent to a dual-output-port intensity modulator. One output of the intensity modulator is fed back to the RF port of the PolM to form an OEO loop. A PD is used in the OEO loop to perform optical-to-electrical conversion. To ensure that the loop gain is higher than unity which is the condition required for oscillation, an electrical amplifier is incorporated. An electrical narrowband bandpass filter (EBPF) is also incorporated in the loop to select the oscillation frequency. The center frequency of the EBPF transmission spectrum is near ω_0. Once the PolM-based OEO is injection locked, a pair of complementary phase-modulated signals is generated along the two principal axes of the PolM. Applying the two phase-modulated signals to Pol2 with its principal axis aligned at 45° to one principal axis of the PolM via tuning the PC (PC4), the phase-modulated signals will be combined to generate an intensity-modulated signal. As a result, a prescaled clock at ω_0 or a line-rate clock at $2\omega_0$ is obtained, depending on the static phase term introduced by PC4.

A. PolM-Based Dual Output Intensity Modulator

Mathematically, the optical field at the output of the PolM along the principal axes (x and y) can be expressed as

$$\begin{bmatrix} E_x \\ E_y \end{bmatrix} = \sqrt{\alpha} E_{\text{in}} \begin{bmatrix} \exp\left(\frac{j}{2}\beta \sin \omega_0 t\right) \\ \exp\left(-\frac{j}{2}\beta \sin \omega_0 t\right) \end{bmatrix} \tag{1}$$

where α is the transmission factor, E_{in} is the input optical field, β is the phase modulation index, and ω_0 is the angular frequency of the OEO oscillating signal. Applying the two signals to a polarizer with its principal axis aligned at 45° to one principal axis of the PolM, we have

$$E_o = \frac{\sqrt{2}}{2}\left[E_x + E_y \cdot e^{-j\phi_B}\right] \tag{2}$$

where ϕ_B is a static phase term introduced by the PC placed before the polarizer. The output optical power is

$$P_{\text{out}} = |E_{\text{out}}|^2 = \alpha |E_{\text{in}}|^2 [1 + \cos(\beta \sin \omega_0 t + \phi_B)]. \quad (3)$$

Dividing P_{out} by the input optical power $P_{\text{in}} = |E_{\text{in}}|^2$, the optical intensity transfer function is obtained, which is written as

$$T = \alpha [1 + \cos(\beta \sin \omega_0 t + \phi_B)]. \quad (4)$$

As can be seen, the transfer function is equivalent to that of an MZM, which is biased at the QTP when $\phi_B = -\pi/2$, or at the MITP when $\phi_B = \pi$. By choosing $\phi_B = -\pi/2$ via tuning PC3 in the OEO loop, the feedback signal at ω_0 for optoelectronic oscillation is obtained. Then, PC4 in the other branch is adjusted to generate optical clocks at ω_0 or $2\omega_0$.

B. Injection Locking of the PolM-Based OEO

It is well known that the modulation spectrum of an ideal return-to-zero (RZ) data signal at a repetition rate of $2\omega_0$ contains no detectable ω_0 component. In a real OTDM data train, however, a small ω_0 component is always observed due to the imperfect multiplexing in the optical domain. In addition, a very small ω_0 component will be occasionally introduced by the optical data in the injection signal or the noise in the OEO. When this RZ signal is launched into the PolM-based frequency-doubling OEO, the weak ω_0 component is converted into an electrical signal by the PD, filtered by the EBPF and amplified by the electrical amplifier. The amplified ω_0 component is then fed back into the PolM-based intensity modulator and modulates the later injected optical data signal. With the modulation, the ω_0 component in the electrical modulation signal and the $2\omega_0$ component in the optical signal will mix at the PolM to generate a new ω_0 component, which would greatly enhance the existing ω_0 component. This positive feedback process would finally lead to an oscillation at the frequency of ω_0 and thus a clock at ω_0 is obtained.

Typically, the clock component in a data signal is more than 10-dB over other components. Considering that the 3-dB passband $\Delta f_{3\text{ dB}}$ of the EBPF is very narrow ($\Delta f_{3\text{ dB}} \leq 50$ MHz), we can simply represent the injection signal as the sum of a dc and two sinusoidal components

$$p(t) \approx p_0 [1 + m_0 \sin \omega_0 t + m_1 \sin(2\omega_0 t + \phi_0)] \quad (5)$$

where p_0 is the average optical power, $m_n (n = 0, 1)$ is the modulation depth and ϕ_0 is the phase of the $2\omega_0$ component relative to that of the ω_0 component in the injection signal. Because the repetition rate of the data signal is $2\omega_0$, the amplitude of the $2\omega_0$ component is much greater than that of the ω_0 component, i.e., $m_0 \ll m_1 \leq 1$.

Assume that the free-running frequency of the OEO is ω_1 ($\omega_1 = \omega_0 + \Delta\omega$ and $\Delta\omega$ is less than the locking range of the OEO), the electrical signal at the modulation port of the modulator before the injection of the data signal can be written as

$$V(t) = V_0 \sin(\omega_1 t + \phi_1). \quad (6)$$

where V_0 is the amplitude and ϕ_1 is the initial phase. Then, in the first cycle after the injection of the data signal, the free-running signal and the injection optical signal will be mixed at the PolM-based intensity modulator. Considering that the output port of the modulator in the OEO loop is biased at the QTP, the optical output signal is given by

$$p_{\text{out}}(t) = \alpha \left[1 + \sin \frac{\pi V(t)}{V_\pi}\right] p(t) \quad (7)$$

where $V\pi$ is the half-wave voltage of the PolM. If the injection signal is a CW light wave, i.e., $m_n = 0$, the OEO is operating at the free running mode. As a free running eigenmode, the ω_1 term must satisfy the following relations:

$$V_0 = 2\alpha p_0 \rho R G J_1(\beta_0) \quad (8a)$$

$$\omega_1 \tau = 2N\pi \quad (8b)$$

where ρ is the responsivity of the PD, R is the load impedance, G is the voltage gain of the amplifier, $\beta_0 = \pi V_0 / V\pi$ is the phase modulation index of the PolM-based intensity modulator, τ is the total loop delay, and N is an integer.

Equation (7) can be expanded in terms of Bessel functions of the first kind, (see (9) at the bottom of the page) where $J_n(x)$ represents the nth-order Bessel functions of the first kind. As can be seen, the optical output signal contains frequency components of $n\omega_0$, $(2k+1)\omega_1$ and $(2k+1)\omega_1 \pm n\omega_0$ (k is an integer, $n = 1, 2$). Because high-order harmonics will be blocked by the narrow bandpass filter, only the components of ω_0, ω_1 (i.e., $\omega_0 + \Delta\omega$), $2\omega_0 - \omega_1$ (i.e., $\omega_0 - \Delta\omega$), and $3\omega_1 - 2\omega_0$ (i.e., $\omega_0 + 3\Delta\omega$) would be present in the obtained electrical signal. In comparison with the ω_1 component, the $\omega_0 - \Delta\omega$ and $\omega_0 + 3\Delta\omega$

$$\begin{aligned} p_{\text{out}}(t) = \alpha p_0 \Bigg[& 1 + m_0 \sin \omega_0 t + m_1 \sin(2\omega_0 t + \phi_0) + 2 \sum_{k=0}^{\infty} J_{2k+1}(\beta) \sin[(2k+1)(\omega_1 t + \phi_1)] \\ & + 2m_0 \sum_{k=0}^{\infty} J_{2k+1}(\beta) \sin[(2k+1)(\omega_1 t + \phi_1) \pm \omega_0 t] \\ & + 2m_1 \sum_{k=0}^{\infty} J_{2k+1}(\beta) \sin[(2k+1)(\omega_1 t + \phi_1) \pm (2\omega_0 t + \phi_0)] \Bigg] \end{aligned} \quad (9)$$

components are very small and should be suppressed after several cycles when the OEO is injection locked. Thus, we only need to consider the ω_0 and ω_1 terms, which is

$$p'_{\text{out}}(t) = \alpha p_0 \left[2J_1(\beta)\sin(\omega_1 t + \phi_1) + m_0 \sin \omega_0 t\right]. \quad (10)$$

The output optical signal is then converted into an electrical signal at the PD, amplified by the electrical amplifier, and filtered by the EBPF, which takes the form of

$$V_1(t) \approx \frac{\beta_1 V_\pi}{\pi}\left[\sin(\omega_1 t + \phi_1) + r_1 \sin(\omega_0 t + \varphi_1)\right] \quad (11)$$

where

$$\beta_1 = \frac{2\pi\alpha p_0 \rho R G J_1(\beta_0)}{V_\pi} \quad (12a)$$

$$r_1 = \frac{1}{2J_1(\beta)} m_0 \quad (12b)$$

$$\varphi_1 = \Delta\omega\tau. \quad (12c)$$

Because the locking range of an OEO-based clock recovery scheme is usually less than 1 MHz [3], [25] and the 3-dB passband of the EBPF is greater than 10 MHz, we simply assume that the loop gains for the ω_0 and ω_1 components are the same.

When the electrical signal in (11) is fed into the PolM-based intensity modulator again, using a similar mathematical treatment as used in deriving (10), after iterating for n times, we can get the expression for the electrical signal generated in the $(n+1)$th cycle, given by

$$V_{n+1}(t) \approx \frac{\beta_{n+1} V_\pi}{\pi} \times \left[\sin(\omega_1 t + \phi_1) + r_{n+1}\sin(\omega_0 t + \varphi_{n+1})\right] \quad (13)$$

where

$$\beta_{n+1} = \frac{2\pi\alpha p_0 \rho R G}{V_\pi} \times \left[J_1(\beta_n) J_0(r_n\beta_n) + m_1 J_1(\beta_n) J_2(r_n\beta_n)\sin(\phi_0 - 2\varphi_n)\right] \quad (14a)$$

$$r_{n+1} = \frac{2\pi\alpha p_0 \rho R G \sqrt{A(\beta_n, r_n, \varphi_n)^2 + B(\beta_n, r_n, \varphi_n)^2}}{\beta_{n+1} V_\pi} \quad (14b)$$

$$\varphi_{n+1} = \Delta\omega\tau + \arctan\left[\frac{B(\beta_n, r_n, \varphi_n)}{A(\beta_n, r_n, \varphi_n)}\right]. \quad (14c)$$

In the above expressions

$$A = m_0 + 2J_0(\beta_n) J_1(r_n\beta_n)\cos\varphi_n + m_1 J_0(\beta_n) \cdot \left[J_1(r_n\beta_n)\sin(\varphi_n - \phi_0) + J_3(r_n\beta_n)\sin(\phi_0 - 3\varphi_n)\right] \quad (15a)$$

$$B = 2J_0(\beta_n) J_1(r_n\beta_n)\sin\varphi_n + m_1 J_0(\beta_n) \cdot \left[J_1(r_n\beta_n)\cos(\varphi_n - \phi_0) + J_3(r_n\beta_n)\cos(\phi_0 - 3\varphi_n)\right]. \quad (15b)$$

Equations (11)–(15) form the framework of the injection-locking theory for the PolM-based frequency-doubling OEO. Using this theory, we can calculate the power evolution of the free running frequency ω_1 and the clock frequency ω_0 when a data signal is injected. The calculation is performed with the parameters used in the experiment: $\beta_0 = 0.45\pi$, $\Delta\omega = 2\pi \times 10^6$, $\tau = 300$ ns, $m_0 = 0.001$, $m_1 = 0.5$, $\phi_0 = 0.5\pi$. To ensure the convergence in the simulation, the saturation of the electrical amplifier is considered. Fig. 2 shows the calculation result. As can be seen, the power of the ω_0 component is very small at the beginning when the OEO is operating at the free-running mode. After only 40 cycles, the ω_1 component is significantly suppressed and the OEO is injection locked at ω_0. In the calculation, the injection locking is always achieved when ϕ_0 is varied from 0 to 2π.

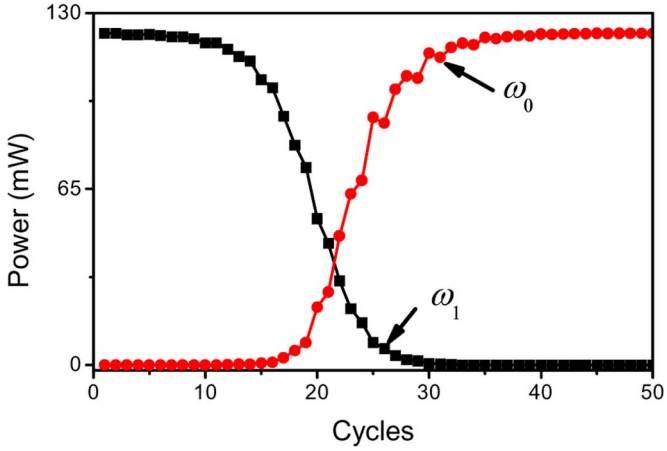

Fig. 2. Power evolution of the free running frequency ω_1 and the clock frequency ω_0 after injection of the data signal.

It is noteworthy that the existence of the ω_0 component is essential for the injection locking. If $m_0 = 0$, i.e., only the $2\omega_0$ component exists in the injection signal, the ω_0 component will never be generated and the OEO can never be injection locked. However, the optical data in the injection signal or the noise in the OEO will occasionally introduce a very small ω_0 component. Once the ω_0 component is present, it will be captured and amplified by the OEO and will lead to a sustained oscillation at the frequency of ω_0. In a calculation, we set $m_0 = 10^{-9}$ in the first cycle and $m_0 = 0$ in the following cycles, injection locking is obtained after 90 cycles. This analysis is in consistence with a previously reported experiment in [26], where a clock division using an OEO is obtained with no SH tone observed in the injection signal.

C. Steady State Analysis

When the OEO is operating in the injection-locked mode, all the free-running modes are suppressed and only the ω_0 component exists. Therefore, it is reasonable to write the electrical signal at the modulation port of the modulator as

$$V'(t) = V_{ph}\sin\left[\omega_0(t - \tau) + \phi'\right]. \quad (16)$$

where ϕ' is the initial phase.

The electrical signal of the OEO and the injection signal will be mixed at the PolM-based intensity modulator, generating frequency components at $k\omega_0 (k = 1, 2, \ldots)$. Because the higher-order harmonics will be blocked by the narrow bandpass filter, we only need to consider the ω_0 component, which is

$$p^{\omega_0}(t) = p_0\alpha\left[A(\beta, \phi)\sin\omega_0 t + B(\beta, \phi)\cos\omega_0 t\right] \quad (17)$$

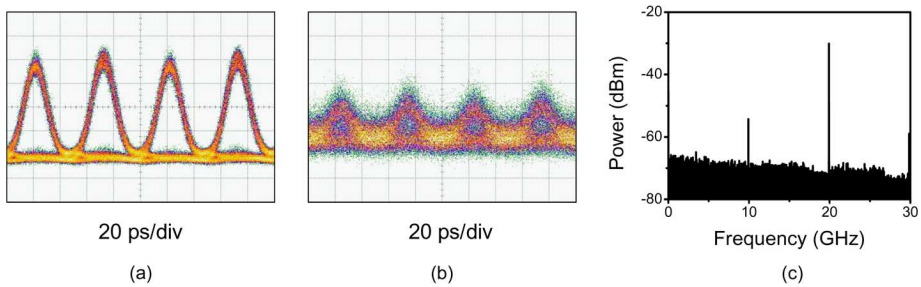

Fig. 3. (a) Eye diagram of the original 20-Gb/s signal, (b) eye diagram, (c) electrical spectrum of the degraded signal.

where

$$A = 2J_1(\beta)\cos\phi + m_0 + m_1\left[J_1(\beta)\sin(\phi-\phi_0) + J_3(\beta)\sin(\phi_0-3\phi)\right] \tag{18a}$$

$$B = 2J_1(\beta)\sin\phi + m_1\left[J_1(\beta)\cos(\phi-\phi_0) + J_3(\beta)\cos(\phi_0-3\phi)\right]. \tag{18b}$$

The output optical signal is then converted into an electrical signal at the PD, amplified by the electrical amplifier, and filtered by the EBPF, which takes the form of

$$V'(t) = V_{ph}\sin\left[\omega_0(t-\tau)+\phi'\right] \tag{19}$$

where

$$V_{ph} = \alpha p_0 \rho R G\sqrt{A^2+B^2} \tag{20a}$$

$$\phi' = \arctan\left(\frac{B}{A}\right). \tag{20b}$$

If the steady state of injection locking is achieved, the feedback signal must be an exact replica of the initial signal represented by (16). Therefore, we obtain

$$\frac{\pi V_{ph}}{V_\pi} = \beta \tag{21a}$$

$$\Delta\omega\tau = \phi - \phi' + 2N\pi. \tag{21b}$$

Because (21) contains special functions, it is very hard to obtain an analytical solution except for some specific cases. Fortunately, numerical approaches, such as iteration method with proper initialization, can obtain β and ϕ for the OEO oscillation signal in (16) if the optical injection signal in (5) is given. If $m_1 = m_0 = 0$, which means a CW signal is injected, from (18)–(21), $\Delta\omega$ must be 0 (i.e., $\omega_1 = \omega_0$), indicating that the OEO operates at the free running mode. Otherwise, the OEO is injection locked at the SH frequency of the injection signal. The oscillation electrical signal is extracted from the $2\omega_0$ component in the data signal since m_0 is very small. Furthermore, one can learn from (18) that the existence of the ω_0 component in the injection signal is not necessary to maintain the oscillation although it is very important for the startup of the injection locking.

On the other hand, if a given pair of (β,ϕ) satisfies (21a), then by substituting (β,ϕ) into (20b) and (21b), the offset frequency from the free running eigenmode represented by $\Delta\omega$ would be obtained [3]. The variable range of $2\Delta\omega$ is defined as the locking range. From (21b), the locking range is inversely proportional to the total loop delay τ and distributed around the free running frequency ω_1. In addition, several locking band would be presented since N can be different values. It is worth mentioning that the difference in loop gain for different frequency is not considered in the treatment. In fact, the injection locking would not be obtained if $\Delta\omega$ is too large to make the loop gain less than unity. With the parameters used in the experiment, the locking range is calculated to be 1.03 MHz for $N = 0$.

III. Experiment and Discussions

An experiment is performed based on the setup shown in Fig. 1. A 9.95328 GHz ($\sim$ 10 GHz) optical pulse train with a pulse width of about 17 ps is generated through electrooptic phase modulation and linear chirp compensation [27]. The center wavelength of the optical pulse is 1556 nm. The pulse train is injected into a $\mathrm{LiNbO_3}$ modulator, where it is modulated by a 9.95328-Gb/s pseudo random bit sequence (PRBS) with a word length of $2^{31}-1$. The obtained 10-Gb/s optical RZ signal is then multiplexed by a passive fiber multiplexer to form a 20 Gb/s OTDM train, with the eye diagram shown in Fig. 3(a). A section of 10-km standard single mode fiber (SSMF) and ASE noise from an erbium-doped fiber amplifier (EDFA) is used to degrade the 20-Gb/s signal. The waveforms and the electrical spectrum of the degraded signal are shown in Fig. 3(b) and (c). A strong 20 GHz component and a small 10 GHz component are present in the electrical spectrum, which are more than 10 dB over other components.

The degraded data signal with a power of 6 dBm and a CW light wave with a power of -3 dBm and a wavelength of 1548.85 nm are fiber coupled into the PolM-based frequency doubling OEO for clock recovery. The PolM is a commercially available 40-Gbit/s GaAs-based PolM from Versawave Technologies [28]. Two polarizers (Pol1 and Pol2) are connected to the PolM via two PCs (PC3 and PC4) to form a dual-output-port intensity modulator. One output of the intensity modulator is connected to the RF port of the PolM, to form an optoelectronic loop. The parameters of the devices used in the OEO loop are as follows: the PD has a 3-dB bandwidth of 45 GHz and a responsibility of 0.4 A/W. The bandwidth of the EBPF is 50 MHz centered at 9.95328 GHz. The power gain of the electrical amplifier is about 55 dB. The free spectral range (FSR) of the OEO is measured to be 3.5 MHz. The other output of the dual-output-port intensity modulator is connected to an optical bandpass filter (OBPF) with a center wavelength of

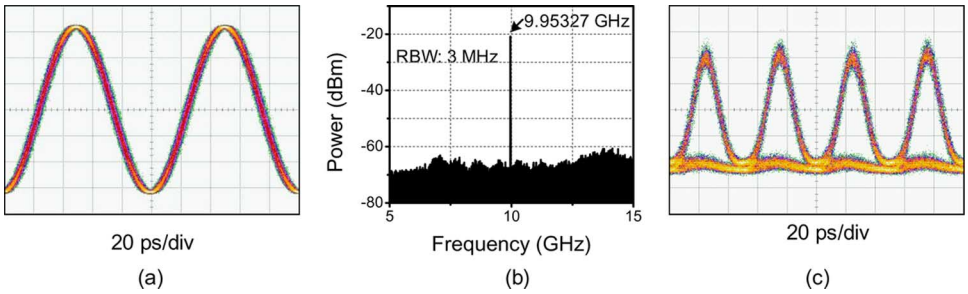

Fig. 4. (a) Waveform and (b) spectrum of the extracted electrical signal. (c) Waveform of the 20 Gb/s signal triggered by the OEO oscillating signal.

1548.85 nm. A prescaled clock at 10 GHz or a line-rate clock at 20 GHz is obtained depending on the static phase introduced by PC4.

To evaluate the performance of the generated optical clocks, a second 45-GHz PD is connected at the output of Pol2, to convert the optical signals to electrical signals. The waveforms are observed by a high-speed sampling oscilloscope (Agilent 86116A) and the spectra are measured by an electrical spectrum analyzer (ESA, Agilent E4448A). In addition, an optical spectrum analyzer (Ando AQ 6317B) with a resolution of 0.01 nm is employed to monitor the optical spectra.

To extract the prescaled or the line-rate clocks from the injection signals, at the first step, the OEO must be injection locked and produce an electrical prescaled clock signal at 10 GHz. To do so, we adjust PC3 in the OEO loop to let $\phi_B = -\pi/2$. Fig. 4(a) and (b) shows the waveform and spectrum of the OEO oscillating signal. The frequency is 9.95327 GHz, which is half the repetition rate of the injection signal within the instrumental error. To demonstrate that the OEO is operating at the injection locking mode, the OEO oscillating signal is served as a trigger for the sampling oscilloscope. Fig. 4(c) shows the 20 Gb/s data monitored with the sampling oscilloscope. The eye pattern is widely open, and almost the same as that in Fig. 3(a), indicating that the incoming data is well synchronized to the recovered clock. Because the 10 GHz component in the injection signal is 20 dB lower than that of the 20 GHz component, the obtained electrical clock is recovered from the 20 GHz component. In the experiment, we slightly vary the polarization states of the incident light wave via adjusting PC1 and find no observable changes to the waveforms and spectra, demonstrating that the oscillation is very robust. In addition, the PRBS length is switched from $2^{31}-1$ to 2^7-1, again, no sensible changes are observed, indicating that the pattern effect does not occur in the experiment. The injection locking status is maintained when the degraded signal is injected. A drop of the 10 GHz clock is observed, but the power variation is within 1 dB. The reason that the OEO possesses sufficient tolerance to the long sequences of '0's or the degradation of the input signal is that the OEO is a oscillator with a high Q factor, which has a high sensitivity to be injection locked.

The locking range of the proposed system is also investigated. It is reported in [3] that the locking range of an OEO is dependent on the phase bias of the modulator. When the phase bias of the PolM-based intensity modulator is $-\pi/2$, the locking range is measured to be 1.32 MHz, which is in good agreement with the theoretical analysis (1.03 MHz). When PC3 is adjusted, which means that the phase bias is deviating from $-\pi/2$, the locking range is increased. The maximum locking range is as large as 27 MHz. Furthermore, as predicted by (21), the OEO is found to have several locking bands, which are

(19.88012 GHz, 19.88286 GHz);
(19.88748 GHz, 19.89248 GHz);
(19.89434 GHz, 19.92138 GHz);
(19.92306 GHz, 19.92806 GHz);
(19.93158 GHz, 19.93582 GHz).

It should be noted that the power of the OEO oscillation signal is reduced (about 2 dB at ~ 19.90 GHz) and the noise is increased when the PolM-based modulator is not biased at the QTP. Therefore, PC3 in the OEO loop is adjusted to let $\phi_B = -\pi/2$ in the following experiments.

To generate the prescaled optical clock, we adjust PC4 in the output port to let $\phi'_B = -\pi/2$, with the main results shown in Fig. 5. Fig. 5(a) shows the optical spectrum, which is a double-sideband modulated optical signal with a wavelength spacing of 0.08 nm or 10 GHz between two neighboring wavelengths. By applying the optical signal at the PD, a sinusoidal signal at 10-GHz is generated, with the temporal waveform shown in Fig. 5(b). Fig. 5(c) gives the spectrum of the generated electrical clock after optical-to-electrical conversion at the PD. Since the PC is tuned to generate the prescaled optical clock, the spectral component of the 10-GHz signal is 26-dB higher than that of its second harmonic. The inset in Fig. 5(c) provides a zoom-in view of the spectral component at 10 GHz.

To generate the line-rate optical clock at 20-GHz, PC4 is adjusted such that $\phi'_B = \pi$. Fig. 6(a) shows the optical spectrum, which is an intensity-modulated signal with suppressed even-order sidebands. As can be seen, the two first-order sidebands are 30-dB higher than the optical carrier and the second-order sidebands. Excellent even-order sideband suppression is confirmed. The wavelengths of the two first-order sidebands are at 1548.772 and 1548.932 nm, giving a wavelength spacing of 0.16 nm or 20 GHz. Fig. 6(b) shows the generated clock with a frequency of 20 GHz. The electrical spectrum of the 20-GHz clock is shown in Fig. 6(c). Although the first and third-order harmonics in the generated microwave signal are observed in the spectrum, they are 24-dB lower than that of the 20-GHz clock. The inset of Fig. 6(c) provides a zoom-in view of the electrical spectrum of the 20-GHz signal.

The key feature of this technique is that no dc bias is needed, which makes the system free from bias drifting, leading to an increased stability. To verify this conclusion, we allow the system to operate at a room environment for a period of 60-min. The

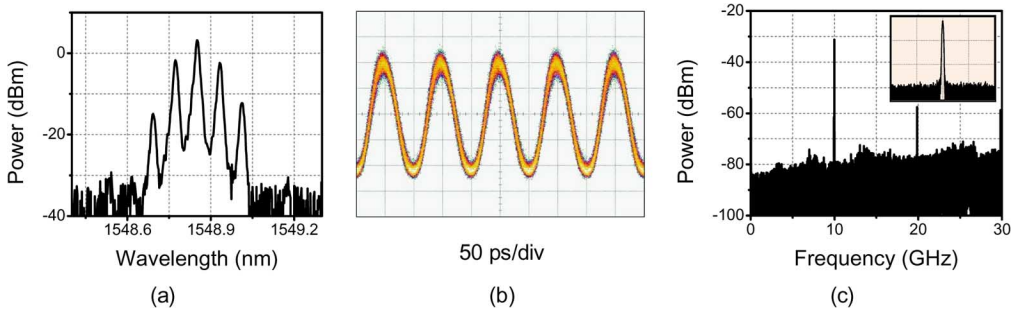

Fig. 5. A 10-GHz clock extracted from the 20 Gb/s degraded signal using the proposed frequency-doubling OEO. (a) The optical spectrum at the output of Pol2. (b) The electrical waveform. (c) The electrical spectrum at SPAN 30 GHz and RBW 100 Hz. Inset: the 10-GHz electrical spectrum at SPAN 1 MHz and RBW 9.1 kHz, vertical: 20 dB/div.

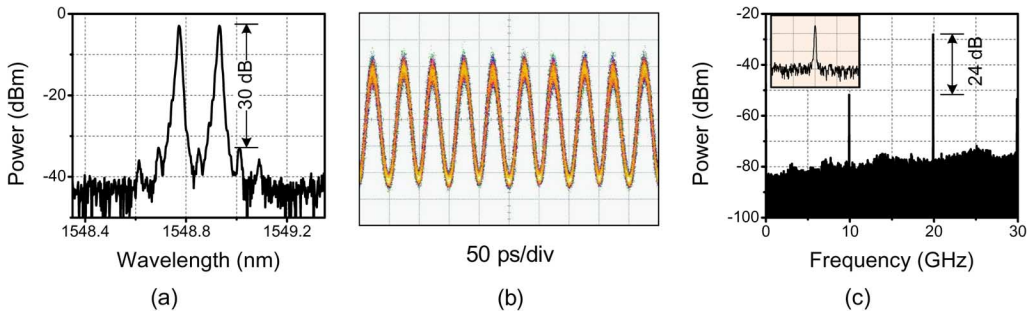

Fig. 6. A 20-GHz clock extracted from the 20 Gb/s degraded signal using the proposed frequency-doubling OEO. (a) The optical spectrum at the output of Pol2. (b) The electrical waveform. (c) The electrical spectrum at SPAN 30 GHz and RBW 100 Hz. Inset: the 20-GHz electrical spectrum at SPAN 1 MHz and RBW 9.1 kHz, vertical: 20 dB/div.

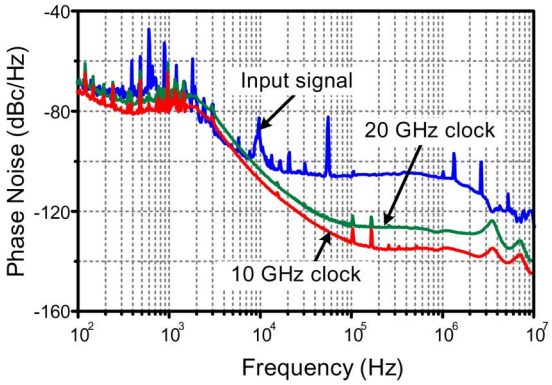

Fig. 7. SSB phase noise spectra for the input signal and the recovered 10- and 20-GHz clocks.

power variations in the optical spectra are within 1 dB. Since the 10-km SSMF used to degrade the injection signal introduces a slowly varied time shift within 7 ps, the temporal waveform is also shifted within 7 ps in the whole observation period, indicating that the recovered clock is synchronized to the injection signal very well.

The phase noise performance of the generated clock signals is also studied. Fig. 7 shows the single-sideband (SSB) phase noise spectra of the generated 10- and 20-GHz clocks, which are measured by an Agilent E5052B signal source analyzer incorporating an Agilent E5053A downconverter. As a comparison, the SSB phase noise spectra for the input 20 Gb/s signal are also plotted. The phase noises at 10-kHz offset frequency are -92.1, -108.8, and -103.1 dBc/Hz for the input OTDM signal, the recovered prescaled clock at 10 GHz, and the recovered line-rate clock at 20 GHz, respectively. The 20-GHz clock has a 5.7-dB phase noise degradation compared to the 10-GHz clock. Theoretically, the phase noise of a frequency-doubled signal should have a phase noise degradation of about $10\log_{10} 2^2 = 6$ dB. The measurement is consistent with the theoretical prediction. A peak at 3.49 MHz offset frequency, corresponding to the FSR of the OEO resulted from the non-oscillating sidemodes, is shown in the SSB phase noise spectra with a phase noise of less than -122 dBc/Hz. Based on the spectral integration method [29] (from 100 Hz to 10 MHz), the rms timing jitters of the 10-GHz and the 20-GHz clocks are estimated to be 192 fs and 154 fs, respectively.

In the above analysis, the injection signal is assumed to have an explicit SH tone. In fact, this SH tone is not required for the proposed clock recovery scheme. This is because a very small SH frequency will be occasionally introduced by the optical data in the injection signal or the noise in the OEO. In another experiment, we replace the EBPF in the OEO loop with another filter that has a center frequency of ~ 6.2 GHz and a 3-dB bandwidth of 20 MHz. The injection signal is also changed to a ~ 12.4 Gb/s RZ data train, which is directly produced by a PRBS with a word length of $2^{31} - 1$. Therefore, the imperfect multiplexing is avoided and no observable 6.2 GHz component is found in the electrical spectrum, as shown in Fig. 8(a). When this signal is injected into the PolM-based OEO, excellent injection locking is again obtained. Fig. 8(b) and (c) shows the waveforms of the recovered prescaled clock at 6.2 GHz and the line-rate clock at ~ 12.4 GHz. Because the 3-dB bandwidth of the EBPF is reduced, only a single locking band is found, which

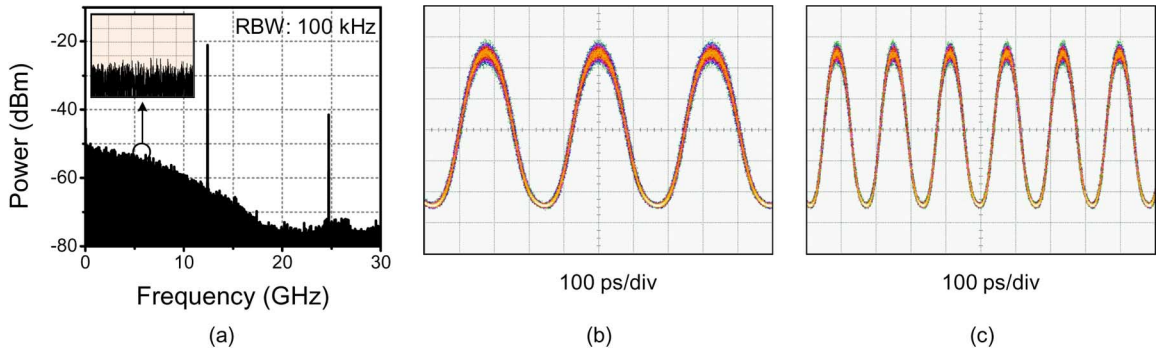

Fig. 8. (a) Electrical spectra of the 12.4 Gb/s signal without explicit subharmonic tone, (b) Waveform of the recovered prescaled clock at 6.2 GHz, (c) Waveform of the recovered line-rate clock at 12.4 GHz.

is (12.37178 GHz, 12.37214 GHz). The locking range is measured to be 360 kHz.

Thanks to the frequency doubling operation of the OEO, to recover the clock from a 20-GHz signal, the devices in the OEO are only required to operate at a maximum frequency of 10-GHz. Therefore, the proposed system can recover both the prescaled clock and the line-rate clock from a 20 Gb/s data signal using only 10-GHz devices. It should be noted that the PolM-based frequency-doubling OEO can be modified to be a frequency-quadrupling OEO. In fact, if PC4 is adjusted to let $\phi_B = 0$, the generated optical signal will be an intensity-modulated signal with suppressed odd-order sidebands. Then, if a notch filter is employed to filter out the optical carrier, an optical microwave signal with a frequency that is four times the frequency of the OEO fundamental signal would be obtained [30]. As a result, the proposed system can be used to extract a prescaled clock and a line-rate clock from a 160 Gb/s data signal if a PolM-based OEO with all 40-GHz devices is applied.

IV. Conclusion

We have proposed and demonstrated a simple and flexible PolM-based frequency-doubling OEO for optical clock recovery from a degraded digital signal. A general mathematical model to describe the injection locking using a low-frequency OEO by a high-speed data signal was developed. Based on the model, the power evolution of different frequency components from a free-running mode to an injection-locked mode was investigated. Injection locking range was obtained by the steady state analysis. An experimental was then performed to verify the proposed scheme. A prescaled optical clock at 10 GHz or a line-rate optical clock at 20 GHz was extracted from a 20 Gb/s degraded optical signal. Clock recovery from a data signal that has no explicit SH tone was also demonstrated. The key significance of the approach is that the use of a low-frequency OEO to realize clock recovery for a high-data-rate signal. For example, by using a 40-GHz OEO, a prescaled clock or a line-rate clock can be extracted from a 160 Gb/s data signal. The proposed approach also features a simple and compact structure with stable operation, which can find applications in optical communications systems.

References

[1] B. Sartorius, "3R all-optical signal regeneration," in *Proc. ECOC'01*, 2001, pp. 98–125.

[2] L. Huo, S. L. Pan, Z. X. Wang, Y. F. Yang, C. Y. Lou, and Y. Z. Gao, "Optical 3R regeneration of 40 Gbit/s degraded data signals," *Opt. Commun.*, vol. 266, no. 1, pp. 290–295, Oct. 2006.

[3] L. Huo, Y. Dong, C. Y. Lou, and Y. Z. Gao, "Clock extraction using an optoelectronic oscillator from high-speed NRZ signal and NRZ-to-RZ format transformation," *IEEE Photon. Technol. Lett.*, vol. 15, no. 7, pp. 981–983, Jul. 2003.

[4] K. Mishina, S. Kitagawa, and A. Maruta, "All-optical modulation format conversion from on-off-keying to multiple-level phase-shift-keying based on nonlinearity in optical fiber," *Opt. Express*, vol. 15, no. 13, pp. 8444–8453, Jun. 2007.

[5] T. Houbavlis, K. E. Zoiros, M. Kalyvas, G. Theophilopoulos, C. Bintjas, K. Yiannopoulos, N. Pleros, K. Vlachos, H. Avramopoulos, L. Schares, L. Occhi, G. Guekos, J. R. Taylor, S. Hansmann, and W. Miller, "All-optical signal processing and applications within the esprit project DO_ALL," *J. Lightw. Technol.*, vol. 23, no. 2, pp. 781–801, Feb. 2005.

[6] S. H. Kim, J. H. Kim, J. W. Choi, C. W. Son, Y. T. Byun, Y. M. Jhon, S. Lee, D. H. Woo, and S. H. Kim, "All-optical half adder using cross gain modulation in semiconductor optical amplifiers," *Opt. Express*, vol. 14, no. 22, pp. 10693–10698, Oct. 2006.

[7] J. P. Turkiewicz, E. Tangdiongga, G. D. Khoe, and H. de Waardt, "Clock recovery and demultiplexing performance of 160-Gb/s OTDM field experiments," *IEEE Photon. Technol. Lett.*, vol. 16, no. 6, pp. 1555–1557, Jun. 2004.

[8] K. Smith and J. K. Lucek, "All-optical clock recovery using a modelocked laser," *Electron. Lett.*, vol. 28, no. 19, pp. 1814–1816, Sep. 1992.

[9] T. Ohno, K. Sato, R. Iga, Y. Kondo, I. Ito, T. Furuta, K. Yoshino, and H. Ito, "Recovery of 160 GHz optical clock from 160 Gbit/s data stream using modelocked laser diode," *Electron. Lett.*, vol. 40, no. 4, pp. 265–267, Feb. 2004.

[10] S. Arahira and Y. Ogawa, "Polarization-insensitive all-optical 160-Gb/s clock recovery with a monolithic passively mode-locked laser diode in polarization-diversity configuration," *IEEE J. Quantum Electron.*, vol. 43, no. 12, pp. 1204–1210, Dec. 2007.

[11] P. E. Barnsley, H. J. Wickes, G. E. Wickens, and D. M. Spirit, "All-Optical clock recovery from 5 Gb/s RZ data using a self-pulsating 1.56 mu-m laser diode," *IEEE Photon. Technol. Lett.*, vol. 3, no. 10, pp. 942–945, Oct. 1991.

[12] I. Kim, C. Kim, G. F. Li, P. L. Wa, and J. Hong, "180-GHz clock recovery using a multisection gain-coupled distributed feedback laser," *IEEE Photon. Technol. Lett.*, vol. 17, no. 6, pp. 1295–1297, Jun. 2005.

[13] T. Ohno, K. Sato, T. Shimizu, T. Furuta, and H. Ito, "Recovery of 40 GHz optical clock from 160 Gbit/s data using regeneratively modelocked semiconductor laser," *Electron. Lett.*, vol. 39, no. 5, pp. 453–455, Mar. 2003.

[14] E. Tangdiongga, J. P. Turkiewicz, G. D. Khoe, and H. de Waardt, "Clock recovery by a fiber ring laser employing a linear optical amplifier," *IEEE Photon. Technol. Lett.*, vol. 16, no. 2, pp. 611–613, Feb. 2004.

[15] H. Dong, H. Z. Sun, G. H. Zhu, Q. Wang, and N. K. Dutta, "Clock recovery using cascaded $LiNbO_3$ modulator," *Opt. Express*, vol. 12, no. 20, pp. 4751–4757, Oct. 2004.

[16] C. Ware, L. K. Oxenlowe, F. G. Agis, H. C. H. Mulvad, M. Galili, S. Kurimura, H. Nakajima, J. Ichikawa, D. Erasme, A. T. Clausen, and P. Jeppesen, "320 Gbps to 10 GHz sub-clock recovery using a PPLN-based opto-electronic phase-locked loop," *Opt. Express*, vol. 16, no. 7, pp. 5007–5012, Mar. 2008.

[17] Z. Y. Hu, H. F. Chou, K. Nishimura, M. Usami, J. E. Bowers, and D. J. Blumenthal, "Optical clock recovery circuits using traveling-wave electroab sorption modulator-based ring oscillators for 3R regeneration," *IEEE J. Sel. Top. Quantum Electron.*, vol. 11, no. 2, pp. 329–337, Mar.-Apr. 2005.

[18] Z. X. Wang, T. Wang, C. Y. Lou, L. Huo, and Y. Z. Gao, "A novel approach for clock recovery without pattern effect from degraded signal," *Opt. Commun.*, vol. 219, no. 1–6, pp. 301–306, Apr. 2003.

[19] X. S. Yao and G. Lutes, "A high-speed photonic clock and carrier recovery device," *IEEE Photon. Technol. Lett.*, vol. 8, no. 5, pp. 688–690, May 1996.

[20] H. Tsuchida, "160-Gb/s optical clock recovery using a regeneratively mode-locked laser diode," *IEEE Photon. Technol. Lett.*, vol. 18, no. 16, pp. 1687–1689, Aug. 2006.

[21] T. Sakamoto, T. Kawanishi, and M. Izutsu, "Optoelectronic oscillator using push-pull Mach-Zehnder modulator biased at point for optical two-tone signal generation," in *Proc. Conf. on Lasers and Electro-Optics, CLEO 2005*, 2005, vol. 2, pp. 877–879.

[22] H. Tsuchida, "Subharmonic optoelectronic oscillator," *IEEE Photon. Technol. Lett.*, vol. 20, no. 17, pp. 1509–1511, Sep. 2008.

[23] M. Shin, V. Grigoryan, and P. Kumar, "Frequency-doubling optoelectronic oscillator for generating high-frequency microwave signals with low phase noise," *Electron. Lett.*, vol. 43, no. 4, pp. 242–244, Feb. 2007.

[24] S. Pan and J. P. Yao, "A frequency-doubling optoelectronic oscillator using a polarization modulator," *IEEE Photon. Technol. Lett.*, to be published.

[25] J. Lasri, P. Devgan, R. Y. Tang, and P. Kumar, "Ultralow timing jitter 40-Gb/s clock recovery using a self-starting optoelectronic oscillator," *IEEE Photon. Technol. Lett.*, vol. 16, no. 1, pp. 263–265, Jan. 2004.

[26] C. Y. Lou, L. Huo, G. Q. Chang, and Y. Z. Gao, "Experimental study of clock division using the optoelectronic oscillator," *IEEE Photon. Technol. Lett.*, vol. 14, no. 8, pp. 1178–1180, Aug. 2002.

[27] T. Otsuji, M. Yaita, T. Nagatsuma, and E. Sano, "10–80-Gb/s highly extinctive electrooptic pulse pattern generation," *IEEE J. Sel. Top. Quantum Electron.*, vol. 2, no. 3, pp. 643–649, Sep. 1996.

[28] J. D. Bull, N. A. Jaeger, H. Kato, M. Fairburn, A. Reid, and P. Ghanipour, "40-GHz electro-optic polarization modulator for fiber optic communications systems," in *Proc. SPIE*, Dec. 2004, vol. 5577, pp. 133–143.

[29] M. Jinno, "Correlated and uncorrelated timing jitter in gain-switched laser-diodes," *IEEE Photon. Technol. Lett.*, vol. 5, no. 10, pp. 1140–1143, Oct. 1993.

[30] S. Pan and J. P. Yao, "Generation of a stable and frequency-tunable microwave signal using a polarization modulator and a wavelength-fixed notch filter," presented at the Opt. Fiber Commun. Conf. Opt. Society of America, 2009, paper JWA51, Technical Digest (CD).

Shilong Pan received the B.S. and Ph.D. degrees in electronics engineering from Tsinghua University, Beijing, China, in 2004 and 2008, respectively.

In August 2008, he joined the Microwave Photonics Research Laboratory, School of information Technology and Engineering, University of Ottawa, Ottawa, ON, Canada, as a Postdoctoral Research Fellow. His current research interests include fiber amplifier and lasers, microwave photonics, optical signal processing and TeraHertz wave generation.

Jianping Yao (M'99–SM'01) received thr Ph.D. degree in electrical engineering from the Université de Toulon, Toulon, France, in 1997.

He joined the School of Information Technology and Engineering, University of Ottawa, ON, Canada, in 2001, where he is currently a Professor, Director of the Microwave Photonics Research Laboratory, and Director of the Ottawa-Carleton Institute for Electrical and Computer Engineering. From 1999 to 2001, he held a faculty position with the School of Electrical and Electronic Engineering, Nanyang Technological University, Singapore. He holds a Yongqian Endowed Visiting Chair Professorship with Zhejiang University, China. He spent three months as an invited professor in the Institut National Polytechnique de Grenoble, France, in 2005. His research has focused on microwave photonics, which includes all-optical microwave signal processing, photonic generation of microwave, mm-wave and THz, radio over fiber, UWB over fiber, fiber Bragg gratings for microwave photonics applications, and optically controlled phased array antenna. His research interests also include fiber lasers, fiber-optic sensors and bio-photonics. He has authored or coauthored over 120 papers in refereed journals and over 100 papers in conference proceedings.

Dr. Yao is a Registered Professional Engineer of Ontario. He is a member of SPIE, OSA and a senior member of the IEEE/LEOS and IEEE/MTT Societies. He received the 2005 International Creative Research Award of the University of Ottawa and was the recipient of the 2007 George S. Glinski Award for Excellence in Research. He was named University Research Chair in Microwave Photonics in 2007. He was a recipient of an NSERC Discovery Accelerator Supplements award in 2008. He is on the Editorial Board of the IEEE TRANSACTIONS ON MICROWAVE THEORY AND TECHNIQUES and an Associate Editor of the *International Journal of Microwave and Optical Technology*.